Report Title:

A Novel Membrane Reactor for Direct Hydrogen Production from Coal

Type of Report: Quarterly Report

Reporting Period Start Date: 4/1/2004

Reporting Period End Date: 6/30/2004

Principal Authors:
Shain Doong, Estela Ong, Mike Atroshenko, Francis Lau, Mike Roberts

Date Report Issued: July 29, 2004

DOE Award Number: DE-FC26-03NT41851

Submitting Organization:
Gas Technology Institute
1700 South Mount Prospect Road
Des Plaines, IL 60018

DISCLAIMER

ABSTRACT

Gas Technology Institute is developing a novel concept of membrane gasifier for high efficiency, clean and low cost production of hydrogen from coal. The concept incorporates a hydrogen-selective membrane within a gasification reactor for direct extraction of hydrogen from coal-derived synthesis gases. The objective of this project is to determine the technical and economic feasibility of this concept by screening, testing and identifying potential candidate membranes under high temperature, high pressure, and harsh environments of the coal gasification conditions. The best performing membranes will be selected for preliminary reactor design and cost estimates.

To evaluate the performances of the candidate membranes under the gasification conditions, a high temperature/high pressure hydrogen permeation unit has been constructed in this project. During this reporting period, the unit has been fully commissioned and is operational. The unit is capable of operating at temperatures up to 1100^{o}C and pressures to 60 atm for evaluation of ceramic membranes such as mixed ionic conducting membrane. A double-seal technique has been developed and tested successfully to achieve leak-tight seal for the membranes. Initial data for a commercial Palladium-Gold membrane were obtained at temperatures to 450C and pressures to 13 atm. Tests for the perovskite membranes are being performed and the results will be reported in the next quarter.

A membrane gasification reactor model was developed to consider the H_2 permeability of the membrane, the kinetics and the equilibriums of the gas phase reactions in the gasifier, the operating conditions and the configurations of the membrane reactor. The results show that the hydrogen production efficiency using the novel membrane gasification reactor concept can be increased by about 50% versus the conventional gasification process. This confirms the previous evaluation results from the thermodynamic equilibrium calculation.

A rigorous model for hydrogen permeation through mixed proton-electron conducting ceramic membranes was also developed based on non-equilibrium thermodynamics. The results from the simulation work confirm that the hydrogen flux increases with increasing partial pressure of hydrogen. The presence of steam in the permeate side can have a small negative effect on the hydrogen flux, in the order of 10%. When the steam partial pressure is greater than 1 atm, the hydrogen flux becomes independent of the steam pressure.

TABLE OF CONTENTS

LIST OF GRAPHICAL MATERIALS

INTRODUCTION

The objective of this project is to develop a novel membrane reactor for high efficiency, clean and low cost production of hydrogen from coal. The concept incorporates a hydrogen-selective membrane within a gasification reactor for direct extraction of hydrogen from coal synthesis gases. This concept has the potential of significantly increasing the thermal efficiency of producing hydrogen and simplifying the processing steps thus reducing the cost of hydrogen production from coal. The specific objective of the project is to determine the technical and economic feasibility of using the membrane reactor to produce hydrogen from coal. GTI and our project team (University of Cincinnati, University of Florida and American Electric Power (AEP)) have identified and will evaluate potential membranes (ceramic and metal) suitable for high temperature, high pressure, and harsh coal gas environments. The best performing membranes will be selected for preliminary reactor design and cost estimates. The overall economics of hydrogen production from this new process will be assessed and compared with other hydrogen production technologies from coal.

Our approach to membrane material screening and testing is to first identify the materials that have good thermal stability under the conditions of gasification temperatures. The candidate membranes will be evaluated for their hydrogen flux in a laboratory permeation unit. The acquired data will provide the basis for a preliminary membrane gasifier design, process development and economic analysis. In the next stage of material screening, chemical stability of the membranes with the syngas and its contaminants generated from coal gasification will be evaluated. The trade-off between the hydrogen permeability and chemical stability will be determined.

As coal gasification for hydrogen production occurs at temperatures above 900^{o}C and pressures above 20 atm, it is critically important to evaluate the hydrogen flux of the candidate membrane materials under these operational conditions. To this end, a high pressure/high temperature permeation unit has been constructed. During this reporting period, the high pressure/high temperature permeation unit has been successfully commissioned. The unit is capable of operating at temperatures and pressures up to 1100^{o}C and 60 atm respectively. The unit will allow screening and testing of the membrane materials at more realistic gasification temperature and pressure conditions. Furthermore, it will be able to demonstrate much higher hydrogen flux from the membranes than what have been reported in the literature.

To support the conceptual design of the membrane gasification reactor, the required size or dimension of the membrane module for a given operating condition must be determined. A modeling approach is used for this task. Modeling on membrane gasification reactor can also identify key parameters that can affect the performance of the membrane gasification reactor. The findings from the modeling results will be discussed in this report.

The mixed proton-electron conducting membrane of the perovskite has been identified as one of the candidate membranes for the gasification applications. To better understand

the transport mechanism for the perovskite membrane, a rigorous model based on non-equlibrium thermodynamics and defect chemistry was formulated. The initial results from this modeling effort are summarized in this report.

EXECUTIVE SUMMARY

During this reporting period, the high pressure/high temperature permeation unit was fully commissioned and is operational. The unit is capable of operating at temperatures up to 1100^{o}C and pressures to 60 atm for evaluation of ceramic membranes such as mixed ionic conducting membranes. A double-seal technique has been developed and tested successfully to achieve leak-tight seal for the membranes. Initial data for a commercial Palladium-Gold membrane were obtained at temperatures to 450C and pressures to 13 atm. Tests for the perovskite membranes are being performed and the results will be reported in the next quarter.

A membrane gasification reactor model was developed to evaluate the H_2 permeability of the membrane, the kinetics and the equilibriums of the gas phase reactions in the gasifier, and the operating conditions and the configurations of the membrane reactor. The results show that the hydrogen production efficiency using the novel membrane gasification reactor concept can be increased by about 50% versus the conventional gasification process. This confirms the previous results from the thermodynamic equilibrium calculation.

A rigorous model for hydrogen permeation through mixed proton-electron conducting ceramic membranes was also developed based on non-equilibrium thermodynamics and defect chemistry. The results from the simulation work confirm that the hydrogen flux increases with increasing partial pressure of hydrogen. The presence of steam in the permeate side can have a small negative effect on the hydrogen flux, in the order of 10%. When the steam partial pressure is greater than 1 atm, the hydrogen flux become independent of the steam pressure in the permeate side.

EXPERIMENTAL

The detailed design of the high pressure permeation was described in the previous reports. The permeation cell was checked for leakage under 1000 psi pressure and was found to hold the pressure quite well. The heater can reach the design temperature of 1100^{o}C. Helium and hydrogen are used as the upstream feed gas while nitrogen is used as the down stream sweeping gas. Gas samples are analyzed by a gas chromatography (HP5890) with a 30-m capillary column packed with molecular sieve 13X. Because it is difficult to separate and detect both hydrogen and helium at the same time by GC, argon is selected as the carrier gas of GC. Helium is also used as the purge gas for the vessel

that encloses the heater. All gas flows are controlled and measured by Brooks mass flow controllers.

Before testing hydrogen-permeation membranes in the high pressure unit, a zirconia membrane which is non-permeable to any gas was first tested to verify the membrane sealing technique. The membrane was positioned at the end of a holding tube with a small section of the inner wall cut off to provide additional seal to the membrane, as shown in Figure 1. The membrane was sealed to the tube using two glass tapes in a shape of O-ring, one above and the other below the membrane. The entire membrane tube assembly was then installed in the permeation unit, first fired to 450C in air to burn out any organic compounds in the glass tapes, followed by N_2 to 950^{o}C. Helium was introduced to the feed side of the membrane while nitrogen was used in the permeate side as a sweeping gas. The permeate gas was sent to GC for analysis and showed no helium in the permeate stream. The system pressure was increased to 20 atm and still no helium could be detected with the GC. This clearly demonstrated that the sealing technique employed in the system could achieve a leak-tight seal for the membrane.

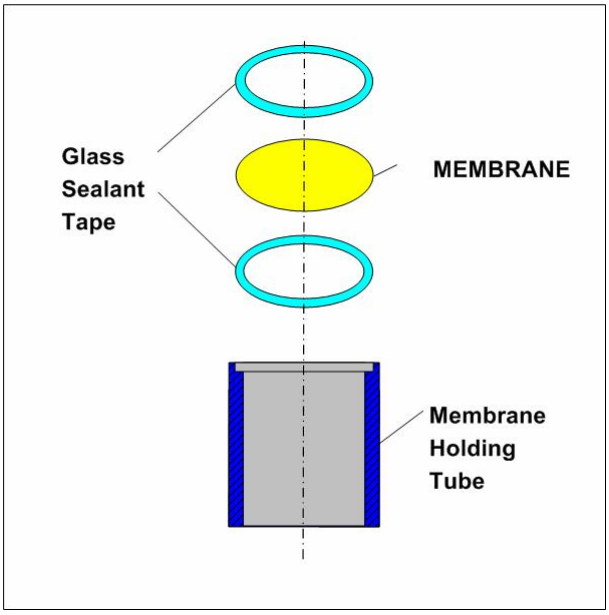

Figure 1. Double-seal design and glass tape provide leak-tight seal for membrane

A $BaCe_{0.8}Nd_{0.2}$ (BCN) membrane made by tape-casting technique with a dense layer thickness of 23 μ and two support layers of 720 μ was tested in the high pressure unit using the same sealing technique. The diameter of the membrane is 2.6 cm. No helium leakage was observed indicating a good seal. When hydrogen was introduced to the feed side of the membrane, however, no hydrogen was detected in the permeate stream. It appeared that the tested membrane did not show any hydrogen permeation. One possible reason of this was the poor porosity of the support layers. More detailed investigation will be conducted.

To further ensure that the high pressure unit is functional, a commercial Palladium-Gold alloy (Pd/Au 80/20) membrane was tested for their hydrogen flux. The membrane was sealed using a high temperature cement and showed no leakage of helium. Hydrogen permeation flux was successfully measured for different temperatures and pressures.

MODELING OF MEMBRANE GASIFICATION REACTOR

To support the conceptual design of the membrane gasification reactor, the required size or dimension of the membrane module for a given operating condition must be determined. The simplified model reported in the previous quarter was improved with a more rigorous approach. A tubular membrane reactor module within a fluidized bed gasifier was used for this modeling study. The free board area or the disengaging zone of a fluidized bed gasifier provides a convenient location for the membrane reactor. Figure 2 is a schematic showing one of the membrane tubes within a fluidized bed gasifier. The coal syngas generated in the gasification zone at the lower section of the fluidized bed enters the membrane reactor module. The membrane tube is assumed to be made of mixed proton/electron conducting perovskite material. Hydrogen will be removed from the tube side of the membrane and the non-permeate will exit the gasifier from the shell side. In this preliminary study, contaminants generated from coal gasification are not considered. In reality, a stable, durable and robust membrane material and the reactor module must be developed.

A mass balance for the feed side of the membrane tube yields

$$\frac{\partial F_i}{\partial x} - R_i + J_i = 0 \qquad (1)$$

where F_i is the molar flow rate of component i, x is the length of the membrane tube, R_i is the reaction rate for forming component i, and J_i is the permeation rate of component i.

To evaluate R_i, chemical kinetics was employed to describe the rates of gas reactions in the feed side of the membrane. This approach was used by Karim and Metwally[1] satisfactorily for modeling of the reforming of natural gas. A reaction scheme comprising 14 chemical species and 32 elemental reaction steps has been employed. The chemical species considered are six major gas components in the gasifier: CH_4, O_2, CO, H_2, CO_2, and H_2O, and eight radicals: OH, CH_3, H, O, HO_2, H_2O_2, CH_2O, and CHO. Because reforming reactions without catalysts are not expected to occur even at the gasification temperature of 1000C, catalytic reaction kinetics was used in the model calculations.

In a simplified form, the hydrogen flux can be expressed in the form of the Wagner equation [2,3]:

$$J_{H_2} = -\frac{RT}{4F^2 L}\frac{(\sigma_{H^+})(\sigma_{el})}{\sigma_{H^+}+\sigma_{el}}\left(\ln(p_{H_2}^f)-\ln(p_{H_2}^p)\right) \qquad (2)$$

where R is the gas constant, F is the Faraday constant, L is the membrane thickness, σ_{H^+} is the proton conductivity, σ_{el} is the electronic conductivity, $p_{H_2}^f$ is the partial pressure of hydrogen in the feed side of the membrane and $p_{H_2}^p$ is the partial pressure of hydrogen in the permeate side.

Equation (1) can be solved with typical numerical techniques. The required boundary conditions are the flow rates and the compositions of the coal syngas entering the membrane tubes. A GTI gasification model U-GAS is used to estimate the gas flow rates and the compositions from a fluidized bed gasifier, which are listed in Table 1 along with other operating conditions and parameters. The Illinois #6 coal is used for this example.

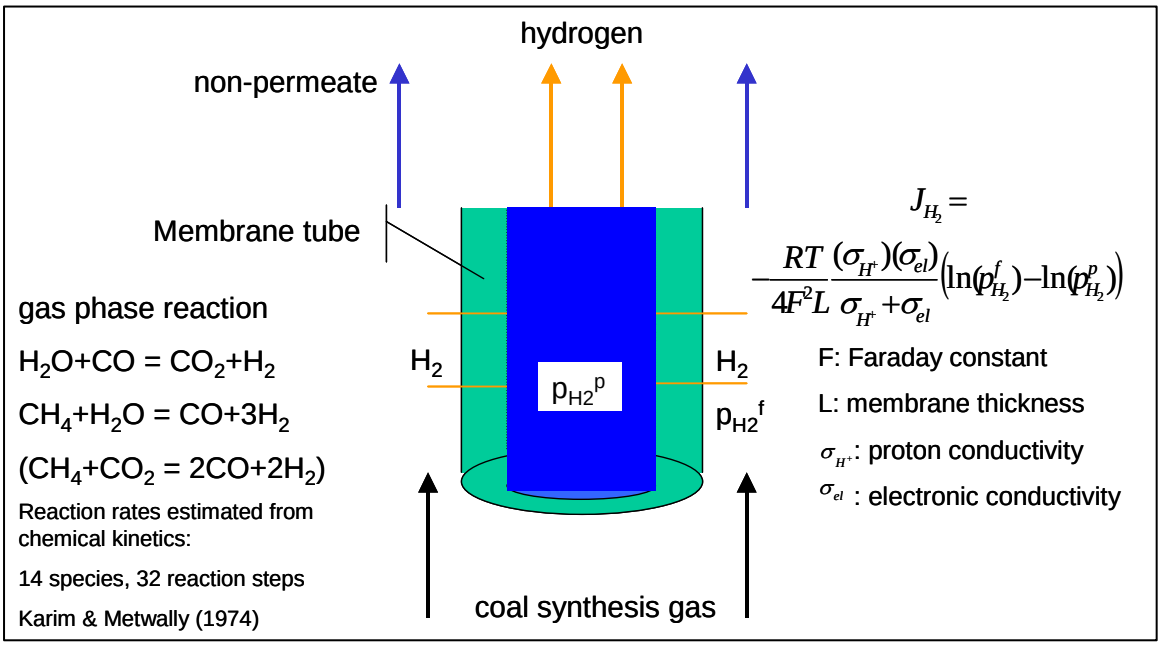

Figure 2. Modeling of a tubular membrane reactor within a gasifier

Table 1. Operating conditions and parameters used in the simulation

coal feed, lb/hr	1000	steam feed to gasifier, lb/hr	595
oxygen feed, lb/hr	534	steam feed to shift reactor,lb/hr	315
temperature, C	1000	coal syngas flow rates, lb/hr	2100
pressure, atm	30	coal syngas composition	
gasifier diameter, cm	50	H_2	0.306
membrane diameter, cm	1.6	CH_4	0.042
membrane thickness, cm	0.002	CO	0.286
membrane length, cm	900	CO_2	0.157
number of membrane tubes	490	H_2O	0.209

MODELING OF MIXED PROTON-ELECTRON CONDUCTING MEMBRANE

A rigorous model for hydrogen permeation through mixed proton-electron conducting ceramic membranes was also developed based on non-equilibrium thermodynamics. The transport of four charged species, proton, oxygen vacancy, electron, and electron hole are described by classical Fick's equation, i.e. flux is proportional to the concentration gradient and the transport coefficient of that species. The concentrations of the species are related to defect chemistry of the perovskite materials and its associated chemical equilibrium. The transport coefficients are determined from the diffusivity, conductivity or mobility measurement. The detailed derivation of the model was given in Appendix.

RESULTS AND DISCUSSION

Hydrogen Permeation Data for Palladium-Alloy Membrane

The commercial Pd-Au membrane tested in the new high pressure unit was 75 micron in thickness. The membrane was sealed using a high temperature cement, heated to 450C. Permeation tests were performed at four temperatures, 450, 400, 350, and 300C at 1 atm. The feed was 50/50 hydrogen/helium with a flow rate of 0.8 SLPM (standard litter per minute). The nitrogen sweeping gas flow was 0.4 SLPM. Operating pressures were also raised to 13 bar at 300C. The data are presented in Figure 3. The hydrogen flux in terms of the permeability are in the order of 2~7 $x10^{-8}$ mole/s/m/$Pa^{1/2}$, which are comparable to the typical hydrogen flux of the palladium membranes reported in the literature [4].

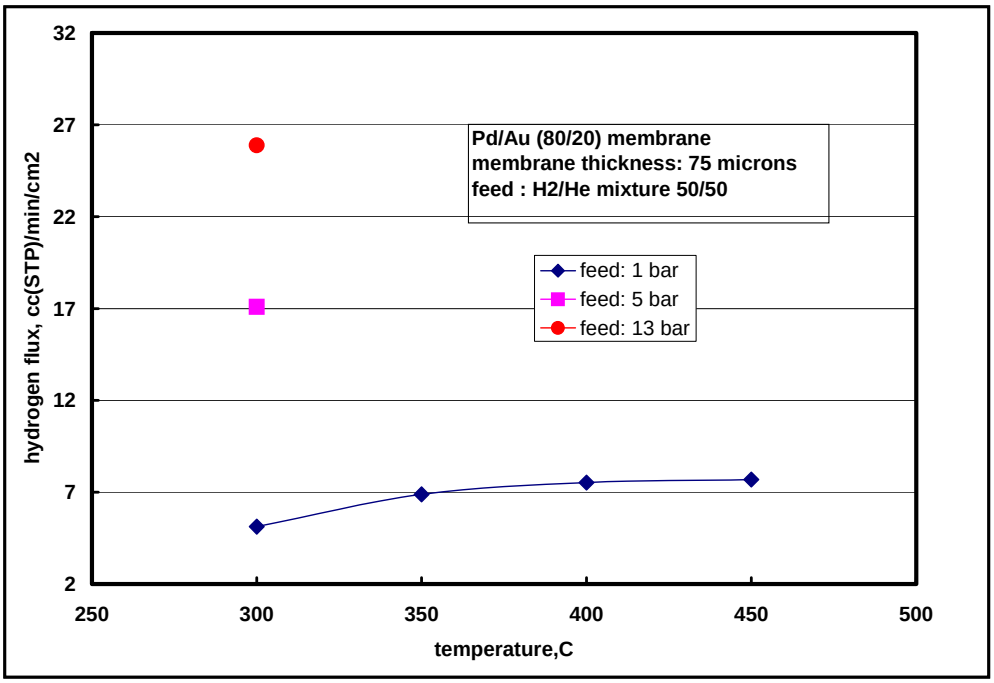

Figure 3. Hydrogen permeation flux for Pd/Au alloy membrane measured from high-pressure permeation unit

Simulation Results for Membrane Gasification Reactor

Simulation was performed for four different process options for hydrogen from coal gasification, as shown in Figure 4. Process A is the conventional coal to hydrogen process, where a Pressure Swing Adsorption (PSA) is used for hydrogen separation unit. Process B combines the shift reaction and hydrogen separation into a single membrane shift reactor unit. Process C is one of the membrane gasification reactor concept, where hydrogen is directly extracted from the coal gasifier and the non-permeable gas, after clean up, is used for power generation. If the non-permeable gas stream is further processed by a membrane shift reactor to increase the overall hydrogen product, this option of the membrane gasification reactor concept is designated as Process D as shown in Figure 4.

For the conventional coal to hydrogen process, Process A, hydrogen recovery for the PSA unit is assumed to be 80%. The shift reaction is assumed to reach equilibrium at 250^{o}C. If a low temperature membrane shift reactor is used as in Process B and D, the hydrogen is removed to such an extent that the partial pressure of hydrogen in the feed side is reduced to slightly above 1 atm and the shift reaction is at equilibrium. The hydrogen partial pressure in the permeate side is maintained at 1 atm, for both the membrane shift reactor and the membrane gasification reactor.

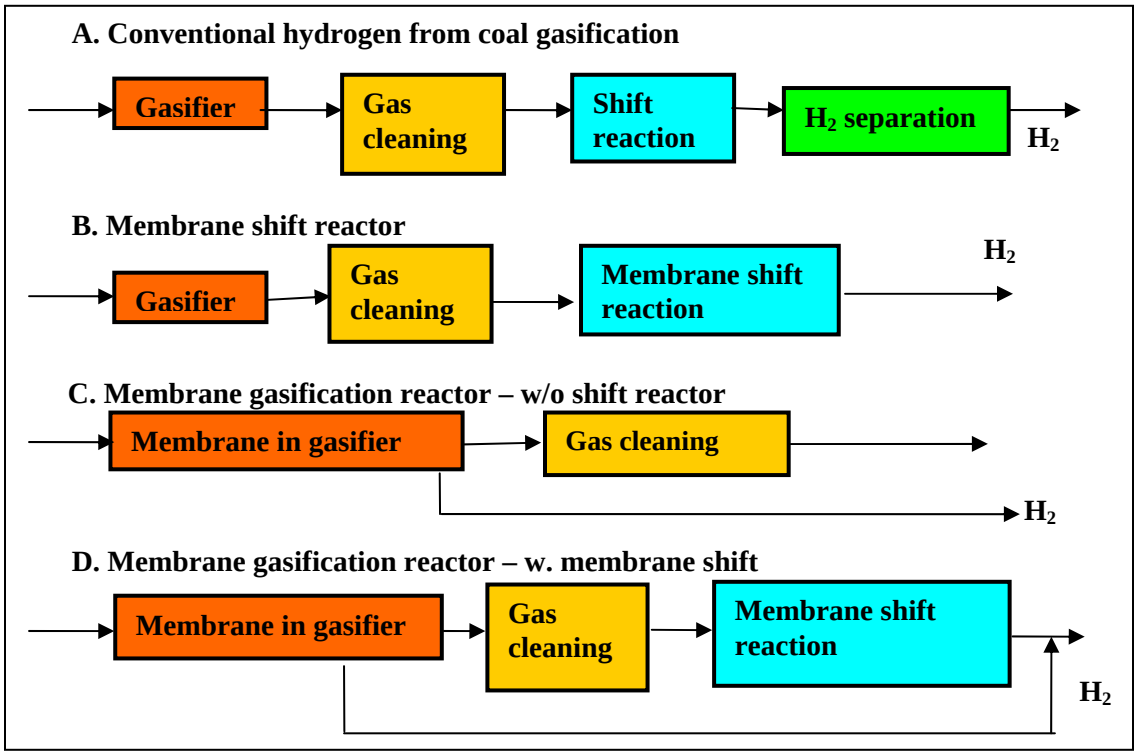

Figure 4. Comparison of Process Options for Hydrogen from Coal Gasification

The results of the simulation are summarized in Table 2 in terms of the number of moles for the hydrogen product and the waste gas or the residual gas. The numbers in Table 2 are all normalized to the hydrogen product for the process A. Process B produces 26% more hydrogen product than Process A because Process B eliminates the hydrogen loss from the PSA tail gas and shifts more CO to H_2 using the membrane shift reactor.

Table 2. Summary of simulation results for the four process options in Figure 4. Catalyzed reactions are assumed for the feed side of the membrane for Process C and D.

Process	A	B	C	D
Hydrogen product, mole	100	126	118	151
Residual gas, mole				
H_2	25	5	6	4
CH_4	9	9	3	3
CO	6	0	33	1
CO_2	92	98	72	103
H_2O	27	21	41	9
to gas clean up	221	221	154	126

As can be seen in Table 2, Process C shows 18% improvement over the conventional process because about two thirds of the methane has been reformed, from 9 to 6. Significant amounts of CO still remain in the non-permeate gas from the membrane

gasification reactor because the shift reaction is less favorable at higher temperatures. If the non-permeable stream is sent to a membrane shift reactor at 250^{o}C, as in Process D, all CO can be converted to H_2 and the overall hydrogen product of Process D will be 51% more than Process A. The results confirm the previous evaluation results from the thermodynamic equilibrium calculation.

The gas flows to the gas clean-up section are also listed at the bottom of the Table 2. Process C and Process D significantly reduce the gas amounts sent to the down stream clean-up section. Because Process C does not use low temperature shift reactor, additional steam is added to the gasifier for Process C so that the overall steam fed to the systems are the same for all four processes. Consequently, the amount of gas to the clean-up section for Process C is higher than Process D.

Concentration profiles along the membrane tube for the gas species in the feed side are plotted in Figure 5. As expected, hydrogen and steam mole fractions decrease while CO_2 mole fraction increases. Methane mole fraction also decreases gradually, indicating occurrence of reforming reaction. CO mole fraction increases because the total gas amount decreases due to the permeation of hydrogen through the membrane. The actual component molar flows are plotted in Figure 6, along with the amount of the hydrogen permeating through the membrane. The actual amount of CO in the feed side decreases due to the shift reaction. However, the conversion of CO is very low, at 22%. The high temperature operation, which is unfavorable to the shift reaction, contributes to the low CO conversion. Shift reaction is almost stopped near the end of the membrane reactor, as CO concentration is at its equilibrium value. Moreover, additional CO is also generated by the reforming reactions of methane. The excess amounts of CO can be converted to more hydrogen, if an additional low temperature membrane shift reactor is used, as in Process D.

Both hydrogen mole fraction and hydrogen molar flow rate approach a constant value in Figure 5 and 6 respectively. Because the pressure of the permeate side is kept at 1 atm, the hydrogen mole fraction in the feed side reaches a pinch point and can not be lower than 3.3% for a 30 atm of feed. Even though significant amounts of CO and steam are still present at the membrane reactor outlet, shift reaction has ceased and attained its equilibrium. Consequently, the hydrogen permeation rate is nearly zero toward the end of the membrane outlet. Obviously, reducing the permeate side pressure can increase the hydrogen flux and promote further CO conversion of the shift reaction.

Simulation Results for Hydrogen Transport in Mixed Proton-Electron Conducting Membrane

Analysis of hydrogen permeation through a mixed proton-electron conducting membrane was carried out using $SrCe_{0.95}Y_{0.05}O_{3-x}$ (SCY) perovskite membrane. The required physical parameters such as diffusivity and equilibrium constants are taken from the literature [5-8]. Typical concentration profiles for the four major defect species are shown in Figure 7 for a 60/40 hydrogen/steam feed at 20 atm. The permeate side is maintained

at 1 atm hydrogen. As seen from Figure 7, both the proton and the electron species dominate in the SCY membrane and the concentrations of the vacancy and the electron hole are very low. The results are reasonable because hydrogen permeation is mainly carried by both proton and electron while the vacancy and the electron hole are responsible for the oxygen transport. The proton and the electron concentrations decrease from the feed side to the permeate side as expected. On the other hand, the concentrations of both the vacancy and the electron hole are higher at the permeate side than at the feed side due to less reducing condition of the permeate side.

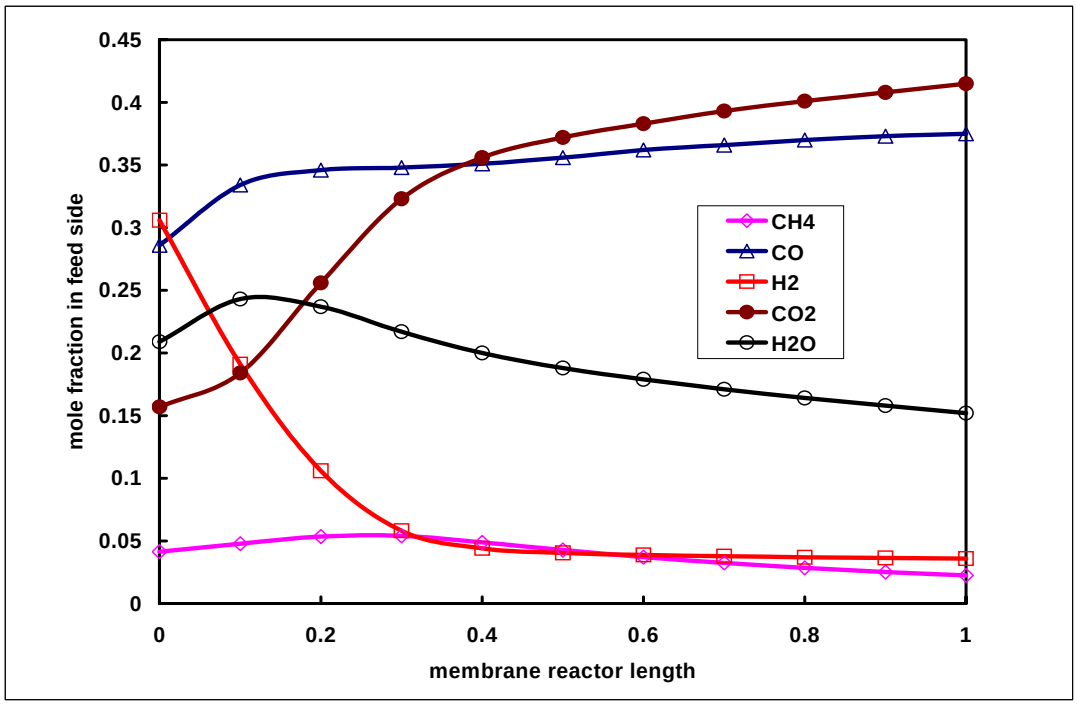

Figure 5. Hydrogen concentration and hydrogen flux at different positions of the membrane as predicted by the model

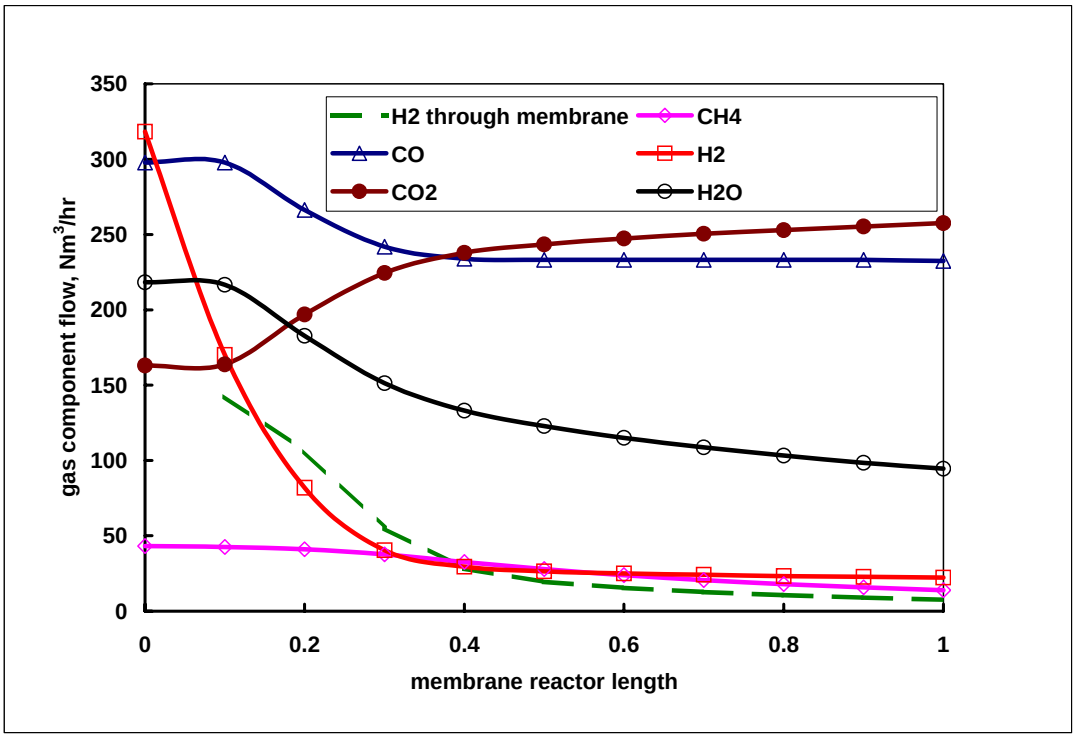

Figure 6. Gas component flow rates in the feed side of the membrane gasification reactor and hydrogen flow through the membrane

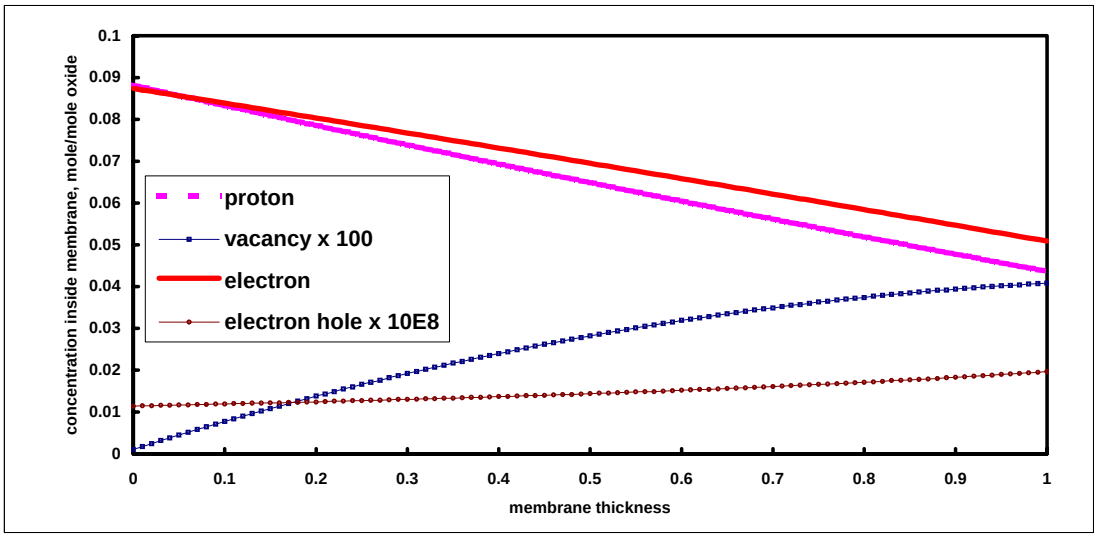

Figure 7. Concentration profiles for the four defect species,, proton, vacancy, electron and electron hole inside a SCY membrane

Simulation was also used to study the effects of the steam partial pressure in the permeate side and the hydrogen partial pressure in the feed side on the hydrogen flux. The presence of steam in the permeate side can reduce the hydrogen flux by about 10% at very dry

conditions. When the steam partial pressure is greater than 1 atm, the hydrogen flux becomes independent of the steam pressure, as shown in Figure 8a. The results from the simulation work confirm that the hydrogen flux increases with increasing partial pressure of hydrogen, as shown in Figure 8b.

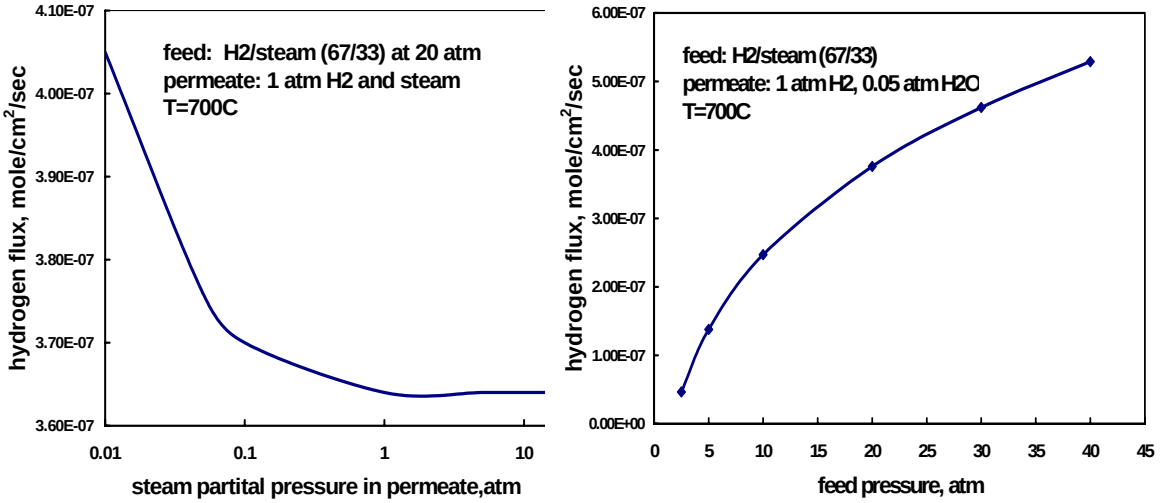

Figure 8. Simulation shows a). the effect of steam partial pressure in the permeate side on hydrogen flux, b) the effect of hydrogen partial pressure in the feed side on hydrogen flux

CONCLUSION

The high pressure/high temperature permeation unit is operational and initial data for the palladium type of membrane have been obtained. The unit is ready to test the perovskite type of membranes at the coal gasification temperature and pressure conditions up to 1100^{o}C and 60 atm respectively. The modeling results show that the hydrogen production efficiency using the novel membrane gasification reactor concept can be increased by about 50% versus the conventional gasification process. A rigorous model for hydrogen permeation through mixed proton-electron conducting ceramic membranes was also developed. This model provides insight on the basic transport mechanism of the proton conducting membranes.

PLAN FOR NEXT QUARTER

Hydrogen permeation testing will be conducted on the new permeation unit under typical gasification temperature and pressure conditions. Current plan will test the following cerate-based perovskite membranes:

- Tri-layered ultra-thin membranes prepared by either tape casting or uniaxially pressing.
- Tri-layered membranes with catalysts incorporated in the support layers.
- Membranes prepared from University of Cincinnati
- Membranes based on perovskite powders supplied from University of Florida
- Dual phase cermet materials incorporating Pd, or Ni in the perovskite structure

The goal of this testing campaign is to determine if the perovskite membranes have sufficient flux for membrane gasifier applications and can be selected for further evaluation for their stability and durability.

REFERENCES

1. G.A. Karim and M.M. Metwally "A Kinetic Investigation of the Reforming of Natural Gas for the Production of Hydrogen", Int. J. Hydrogen Energy, Vol. 5, pp 293, 1979
2. H.J.M. Bouwmeester and A.J. Burggraaf "Dense ceramic membranes for oxygen separation", in Fundamentals of Inorganic Membrane Science and Technology, Ed. By A.J. Burggraff and L. Cot, pp 435-528, 1996, Elsevier Science B.V.
3. T. Norby and Y. Larring "Mixed hydrogen ion-electronic conductors for hydrogen permeable membranes", Solid State Ionics, 136-137, pp139-148, 2000
4. B.D. Morreale,M.V. Ciocco, R.M. Enick, B.I. Morsi, B.H. Howard, A.C. Cugini, K.S. Rothenberger "The permeability of hydrogen in bulk palladium at elevated temperatures and pressures", J. of Membrane Science, 212, pp87-97, 2003
5. X. Tan, S. Liu, K. Li and R. Hughs "Theoretical analysis of ion permeation through mixed conducting membranes and its application on dehydrogenation reactions", Solid State Ionics, 138, pp149-159, 2000
6. L. Li and E. Iglesia "Modeling and analysis of hydrogen permeation in mixed proton-electronic conductors", 58, pp1977-1988, 2003
7. T. Schober, W. Schilling and H. Wenzl "Defect model of proton insertion into oxides", 86-88, pp653-658, 1996
8. S-J Song, E.D. Wachsman, J. Rhodes, S.E. Dorris, U. Balachandran "Numerical modeling of hydrogen permeation in chemical potential gradients", 164, pp107-116, 2003

APPENDIX

In a MIEC membrane, the driving forces for the transport of charged species come from both chemical and electrical potential gradients. The flux of each species k, J_k can be described by a combination of Fick's law and the equation for ion migration:

$$J_k = -\frac{\sigma_k}{z_k^2 F^2}\left(\frac{\partial \mu_k}{\partial x} + z_k F \frac{\partial \phi}{\partial x}\right) \quad \text{(A1)}$$

where μ is the chemical potential, ϕ is the electrical potential, σ is the conductivity, z is the charge number and F is the Faraday constant.

When no external current is imposed on the membrane, the net flux from all the charged species is zero, i.e.

$$I = \sum_{k=1}^{n} I_k = \sum_{k=1}^{n} z_k F J_k = 0 \quad \text{(A2)}$$

Combining Eqs.(A1) and (A2), a relationship between the electrical potential and the chemical potential can be obtained:

$$\frac{\partial \phi}{\partial x} = -\sum_{k=1}^{n} \frac{t_k}{z_k F} \frac{\partial \mu_k}{\partial x} \quad \text{(A3)}$$

where t_k is the transport number of species k, which is a relative measure of conductivity of species k to the total conductivity.

$$t_k = \frac{\sigma_k}{\sum_{i=1}^{n} \sigma_i} \quad \text{(A4)}$$

The flux equation, Eq. (A1) now becomes

$$J_k = -\frac{\sigma_k}{z_k^2 F^2}\left(\frac{\partial \mu_k}{\partial x} - z_k \sum_{i=1}^{n} \frac{t_i}{z_i} \frac{\partial \mu_i}{\partial x}\right) \quad \text{(A5)}$$

Chemical potential μ is related to chemical activity a_i by

$$\frac{\partial \mu_k}{\partial x} = RT \frac{\partial \ln a_k}{\partial x} \tag{A6}$$

Under ideal conditions, the activity a can be substituted with the concentration C. Further, the conductivity of the defect species can be correlated with its concentration and diffusivity by the Nernst-Einstein equation:

$$\sigma_k = \frac{z_k^2 F^2}{RT} C_k D_k \tag{A7}$$

Substituting Eq.(A6) and (A7) into Eq.(A5), the following equation can be obtained:

$$J_k = -C_k D_k \left[\frac{(1-t_k)}{C_k} \frac{\partial C_k}{\partial x} - \sum_{\substack{i=1 \\ i \neq k}}^{n} \frac{z_k t_i}{z_i C_i} \frac{\partial C_i}{\partial x} \right] \tag{A8}$$

Eq. (A8) relates the flux of each species to the concentrations and the diffusivities of all the species inside the MIEC membrane.

In proton-electron conductors, charged carriers are protons ($OH^{\bullet}$), vacancies ($V_{\ddot{O}}$), electrons (e^{-}), and electron holes ($h^{\bullet}$). The concentrations of the defect species in a typical proton conductor can be described by the following stoichiometric equations:

$$1/2 O_2 + V_{\ddot{O}} = O_O^x + 2h^{\bullet} \qquad K_1 = C_h^2 \Big/ \left(C_V \, p_{O_2}^{1/2} \right) \tag{A9}$$

$$H_2 + 2O_O^x = 2OH^{\bullet} + 2e^{-} \qquad K_2 = \left(C_{OH}^2 C_e^2 \right) \Big/ p_{H_2} \tag{A10}$$

$$H_2 + 1/2 O_2 = H_2O \qquad K_3 = p_w \Big/ \left(p_{H_2} \, p_{O_2}^{1/2} \right) \tag{A11}$$

where O_O^x denotes the lattice oxygen. Eqs.(A9) to (A11) establish the relationships between the concentrations of charged species inside the membrane to the gas partial pressures outside the membrane. The chemical potentials of each charged species can also be related to the chemical potentials of gases through the following equations corresponding to Eqs.(A9) to (A11):

$$1/2 \mu_{O_2} + \mu_V = 2\mu_h \tag{A12}$$

$$\mu_{H_2} = 2\mu_{OH} + 2\mu_e \tag{A13}$$

$$\mu_{H_2} + 1/2\mu_{O_2} = \mu_w \tag{A14}$$

Also the electronic equilibrium requires

$$e^- + h^\bullet = nil \qquad K_e = C_e C_h \tag{A15}$$

$$\mu_e + \mu_h = 0 \tag{A16}$$

Therefore, Eq.(A8) for proton $OH^\bullet$ and vacancy $V_{\ddot{O}}$, will become

$$J_{OH} = -\frac{t_{OH}\sigma RT}{2F^2}\left[(t_h + t_e)\frac{\partial \ln p_{H_2}}{\partial x} + 4t_V\sigma\frac{\partial \ln p_w}{\partial x}\right] \tag{A17}$$

$$J_V = -t_V\sigma\frac{RT}{F^2}\left[(t_h + t_e)\frac{\partial \ln p_{H_2}}{\partial \ln x} - (t_h + t_e + t_{OH})\frac{\partial \ln p_w}{\partial x}\right] \tag{A18}$$

Eqs.(A17) and (A18) can not be integrated directly because the transport numbers, t_i and the total conductivity σ are functions of the membrane position x. However, at steady state, J_{OH} and J_V are constant and independent of the membrane positions. The above equations can be rearranged to give

$$\frac{RT}{F^2}\frac{\partial \ln p_{H_2}}{\partial x} = -\frac{4J_V}{\sigma(t_h + t_e)} - \frac{2J_{OH}(t_h + t_e + t_{OH})}{\sigma t_{OH}(t_h + t_e)} \tag{A19}$$

$$\frac{RT}{F^2}\frac{\partial \ln p_w}{\partial x} = \frac{J_V}{\sigma t_V} - \frac{2J_{OH}}{\sigma t_{OH}} \tag{A20}$$

Given the boundary conditions at both the feed side and the permeate side of the membrane, Eqs.(A19) and (A20) can be integrated with respect to x to obtain the profiles of hydrogen and water partial pressures across the membrane. The concentration profiles of the four defect species, proton (C_{OH}), vacancy (C_V), electron (C_e), and electron hole (C_h) are related to the gas partial pressure through Eqs.(A9) to (A11). The required parameters for the membrane material are equilibrium constants, $K_1, K_2, K_3,$ and K_e as well as the diffusivity data for the four defect species.